

Anisotropic electronic structure of the Si(111)-(4×1)In surface

Jun Nakamura,^{1,*} Satoshi Watanabe,² and Masakazu Aono^{1,3,4}

¹Surface and Interface Laboratory, RIKEN, 2-1 Hirosawa, Wako, Saitama 351-0198, Japan

²Department of Materials Science, The University of Tokyo, 7-3-1 Hongo, Bunkyo-ku, Tokyo 113-8656, Japan

³Department of Precision Science and Technology, Osaka University, Suita, Osaka 565-0871, Japan

⁴CREST, Japan Science and Technology Corporation, Kawaguchi Center Building, Hon-cho 4-1-8, Kawaguchi, Saitama 332-0012, Japan

(Received 28 December 2000; revised manuscript received 22 February 2001; published 27 April 2001)

We have investigated the atomic structure and electronic states of the Si(111)-(4×1)In surface using the first-principles total energy calculations. The atomic coordinates optimized for this surface are in excellent agreement with those obtained from the recent x-ray diffraction experiment [Bunk *et al.*, Phys. Rev. B **59**, 12 228 (1999)]. The calculated surface electronic structure, which is anisotropic, provides a satisfactory description of angle-resolved photoemission data. These calculations provide strong support for the model proposed by Bunk *et al.*

DOI: 10.1103/PhysRevB.63.193307

PACS number(s): 68.35.Bs, 73.20.At, 68.43.Bc

In past years, much interest has been devoted to exotic physical phenomena of quasi-one-dimensional (1D) materials on semiconductor surfaces, such as the carbon atomic chain on beta-SiC(100) (Ref. 1), group-III metals on Si(100) (Ref. 2), bismuth on Si(100) (Ref. 3), and cesium on InAs(110) (Ref. 4). In these systems, Peierls-like instabilities and a charge density wave (CDW) characteristic of quasi-1D metals have not yet been observed. Recently, however, Yeom *et al.* have revealed that the electronic structure of self-assembled indium (In) chains on Si(111), i.e., the Si(111)-(4×1)In surface [hereafter referred to as the (4×1)In surface], shows the characteristics of a 1D metallic system:⁵ (1) The Fermi contours of the room-temperature metallic phase measured by angle-resolved photoemission exhibit a perfect nesting; (2) This room-temperature phase undergoes a temperature-induced, reversible transition into a semiconducting (8×2) phase; (3) The 1D CDW along the In chains is observed using a scanning tunneling microscope at low temperature. On the contrary, very recently, Kumph *et al.* have given a negative view of the CDW of this system.⁶ The formation of CDW cannot be the driving force for the phase transition. Moreover, they have concluded that there exist very strong chain-to-chain correlations *only* in the direction perpendicular to the chains.⁶ Thus, opinion is divided among researchers on this subject.

Before turning to a mechanism of the phase transition of this system, we have to investigate the atomic arrangement and electronic states of the (4×1)In surface. In this report, we give the first theoretical investigation of the atomic and electronic structures of the (4×1)In surface using the first-principles total energy and band calculations.

The reconstruction of the (4×1)In surface has been investigated with a variety of techniques such as low-energy electron diffraction,^{7,8} reflection high-energy electron diffraction,^{9–11} impact collision ion-scattering spectroscopy,^{12,13} photoemission spectroscopy,^{14–18} x-ray diffraction (XRD),^{19–21} Auger electron spectroscopy,²² scanning tunneling microscopy,^{23–25} and direct methods of transmission electron diffraction.²⁶ In particular, the atomic arrangement of this surface, as well as the electronic structure, has been extensively debated to date. Recently, a plausible

structural model has been proposed by Bunk *et al.* using surface XRD,²¹ which consistently explains all previously published experimental data. Furthermore, very recently, their model has also been supported by electron diffuse scattering experiments.²⁷ Hence, we focus our attention on the model of Bunk *et al.*²¹ in the present report. Indeed, only on the basis of the Bunk *et al.* model, both optimized atomic structure and calculated dispersions of bands crossing the Fermi level are in excellent agreement with the experimental ones. Another plausible model proposed by Saranin *et al.*²⁵ does not provide a satisfactory description of angle-resolved photoemission data. Thus, our calculations provide strong support for the Bunk *et al.* model.

The theoretical calculations were performed with TAPP (Tokyo Ab initio Program Package).²⁸ The total energy calculations were performed within density functional theory²⁹ in the generalized gradient approximation,^{30,31} using the

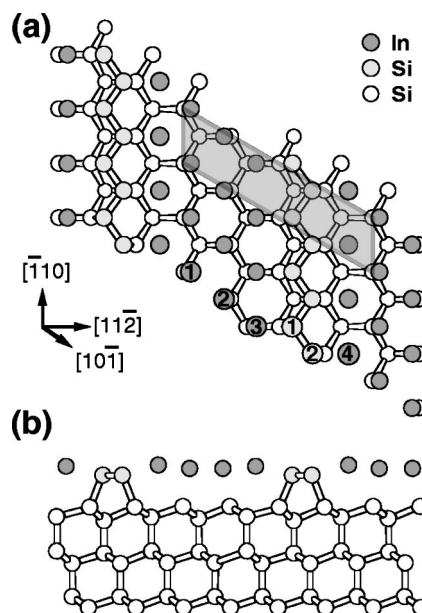


FIG. 1. Top (a) and side (b) views of the optimized geometry for the (4×1)In surface. The (4×1) unit cell is indicated by the shaded area.

TABLE I. Reduced atomic coordinates obtained by the present calculation and experiment (Ref. 21) in reduced coordinates (see text). In column 2, shown are the ideal (bulk-like) positions for comparison. Column 4 shows the difference between measured and calculated atomic positions in (Å).

	Bunk <i>et al.</i> (Ref. 21)	Ideal (bulklike) position	This work	Deviation in (Å)
In(1)	(0.11, 0.06, 0.86)		(0.143, 0.072, 0.843)	~0.12
In(2)	(0.86, 0.93, 0.85)		(0.863, 0.931, 0.857)	~0.02
In(3)	(1.53, 0.77, 0.99)		(1.553, 0.776, 0.981)	~0.08
In(4)	(3.43, 0.22, 0.99)		(3.459, 0.229, 0.992)	~0.10
Si(1)	(2.28, 0.14, 0.73)		(2.297, 0.149, 0.698)	~0.12
Si(2)	(2.71, 0.86, 0.76)		(2.713, 0.856, 0.708)	~0.16
Si	(0.31, 0.65, -0.26)	(0.333, 0.667, -0.250)	(0.331, 0.666, -0.259)	~0.07
Si	(3.96, 0.98, -0.00)	(4.000, 1.000, 0.000)	(4.001, 0.999, 0.002)	~0.14
Si	(1.30, 0.65, -0.25)	(1.333, 0.667, -0.250)	(1.335, 0.668, -0.227)	~0.14
Si	(0.96, 0.98, 0.04)	(1.000, 1.000, 0.000)	(0.994, 0.997, 0.014)	~0.14
Si	(2.29, 0.64, -0.33)	(2.333, 0.667, -0.250)	(2.328, 0.664, -0.305)	~0.15
Si	(2.01, 0.00, -0.03)	(2.000, 0.000, 0.000)	(2.025, 0.012, -0.023)	~0.06
Si	(3.29, 0.65, -0.23)	(3.333, 0.667, -0.250)	(3.326, 0.663, -0.232)	~0.12
Si	(2.95, 0.97, -0.01)	(3.000, 1.000, 0.000)	(2.973, 0.987, -0.007)	~0.08
Si	(0.66, 0.33, -1.24)	(0.667, 0.333, -1.250)	(0.668, 0.334, -1.252)	~0.05
Si	(0.33, 0.67, -1.01)	(0.333, 0.667, -1.000)	(0.332, 0.666, -1.008)	~0.02
Si	(1.65, 0.32, -1.26)	(1.667, 0.333, -1.250)	(1.656, 0.328, -1.260)	~0.03
Si	(1.32, 0.66, -0.99)	(1.333, 0.667, -1.000)	(1.336, 0.668, -0.990)	~0.05
Si	(2.67, 0.33, -1.27)	(2.667, 0.333, -1.250)	(2.670, 0.335, -1.270)	~0.02
Si	(2.32, 0.66, -1.04)	(2.333, 0.667, -1.000)	(2.330, 0.665, -1.046)	~0.04
Si	(3.66, 0.33, -1.25)	(3.667, 0.333, -1.250)	(3.665, 0.332, -1.250)	~0.02
Si	(3.31, 0.65, -0.98)	(3.333, 0.667, -1.000)	(3.330, 0.665, -0.993)	~0.08

scalar-relativistic^{32,33} ultrasoft pseudopotentials.^{34–37} We introduced a partial core correction to the In pseudopotential in order to consider a nonlinear effect for the exchange-correlation term.³⁸ A slab geometry was used for the simple calculation, which has a supercell consisting of six atomic layers of Si, adlayers of Si and In, and a vacuum region corresponding to eight atomic layers in thickness. The back surface of the slab was terminated with four hydrogen atoms that eliminate artificial dangling bonds and prevent it from coupling with the front surface of the slab. The wave functions were expanded in a plane-wave basis set with an energy cutoff of 25.0 Ry. Twenty-five special k points were employed to sample the irreducible Brillouin zone for the (4×1) unit cell. Both electronic and ionic degrees of freedom were optimized using the conjugate gradient method.

The optimized atomic configuration and its coordinates (a, b, c) for the (4×1) In surface are shown in Fig. 1 and Table I, respectively. Here, we adopted reduced atomic coordinates with $a = 1/2[10\bar{1}]_{cubic}$, $b = 1/2[\bar{1}10]_{cubic}$, and $c = 1/3[111]_{cubic}$. The cubic coordinates are in units of the silicon lattice constant, 5.43 Å. In this table, the ideal (bulk-like) coordinates and the results of the surface XRD by Bunk *et al.*²¹ are also shown for comparison. The overall magnitude of the atomic relaxations are in excellent agreement with the surface XRD results. Deviations from the experiments in absolute coordinates are less than ~0.16 Å. The interatomic distances of In(3)-Si(1) and In(4)-Si(2) are 2.63 and 2.64 Å, respectively, which are comparable to the sum of the covalent bond radii of Si and In, 2.61 Å. This means

that the neighboring In atoms on the Si chain, In(3) and In(4), are covalently bonded to the Si atoms in the Si chain. On the other hand, the nearest-neighbor distances between the In atoms are within the range of 3.01~3.07 Å and are slightly shorter than the bulk In value (3.25 Å). This implies that the bondings between In atoms have not only a metallic character but also a covalent one. Figure 2(a) shows the total valence charge density in the (111) plane cutting the topmost In atoms, In(3). As evident in this figure, the valence charges are localized along the bonds for In(3)-Si(1) and In(4)-Si(2), suggesting the covalent nature of those bonds.

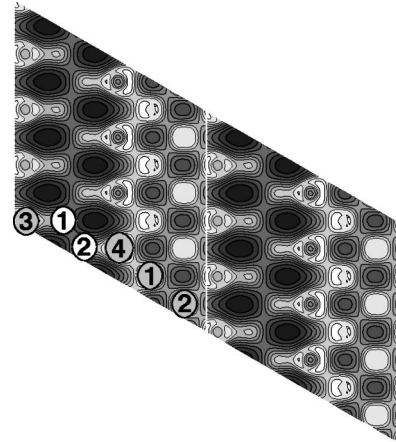


FIG. 2. Total valence charge-density map, which is drawn for the (111) plane including the topmost In atom labeled 4 in Fig. 1.

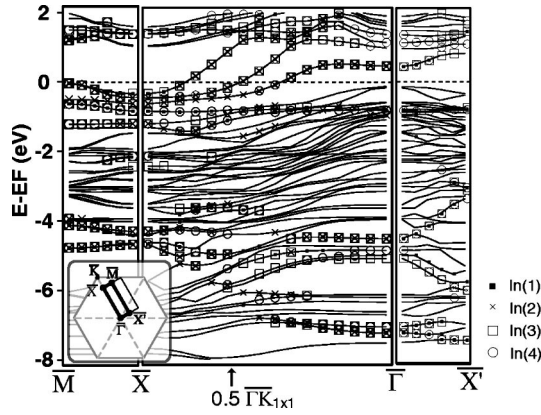


FIG. 3. Band structure of the $(4 \times 1)\text{In}$ surface. Closed square, cross, open square, and open circle denote the orbitals having large amplitudes at In(1), In(2), In(3), and In(4), respectively. Here, the numbers of atoms correspond to those in Fig. 1 and Table I.

Furthermore, the charge distributions between In(1)-In(4) and In(2)-In(3) have directivity to some extent, indicating that two In chains, -In(1)-In(4)-In(1)- and -In(2)-In(3)-In(2)-, are formed as well as the Si chain.

Figure 3 shows the band structure of the (4×1) surface, where various symbols denote the orbitals having large amplitudes at the surface In atoms (see figure caption). In the inset of this figure, the surface Brillouin zones of the $(4 \times 1)\text{In}$ surface are also shown with thick solid lines. In this report, we adopted a rectangular (4×1) Brillouin zone, in which the ΓX and $\Gamma X'$ directions correspond to the directions perpendicular and parallel to the atomic chains, respectively. As is clearly evident, the electronic structure of this surface is strongly anisotropic: There are three metallic bands, $m1$, $m2$, and $m3$, crossing the Fermi level along the ΓX direction, which have large amplitude at the surface In atoms, while along the direction perpendicular to the atomic chain ($\Gamma X'$, XM , and any directions parallel to those) we can see finite-energy band gaps, that is, the electronic structure is semiconducting along this direction. This anisotropic feature of the electronic states has been confirmed by the experiments.^{5,16}

The surface states for the $(4 \times 1)\text{In}$ surface can be classified into three groups; (1) three metallic bands crossing the Fermi level, (2) nearly flat bands at about -1 eV, and (3) parabolically dispersive bands at $-4 \sim -7$ eV. Three metallic states, $m1$, $m2$, and $m3$, are localized at the surface, which consists of In-5 p orbitals and Si-2 p orbitals of substrate Si atoms. Therefore, these states are attributed not only to the metallic bonds in the In overlayer as predicted by Abukawa *et al.*¹⁶ but also to covalentlike bondings between In atoms and substrate Si atoms beneath In(1) and In(2). Next, nearly flat band lying at ~ -1 eV seems to corre-

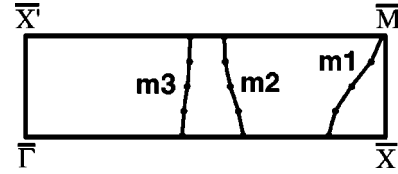


FIG. 4. Calculated Fermi surfaces of the $(4 \times 1)\text{In}$ surface. We plotted the points where three metallic bands cross E_F in the rectangular (4×1) Brillouin zone.

spond to the band d ($d1$ and $d2$) in Ref. 16, which is originated from the localized, covalent bondings between the surface Si and In atoms, i.e., In(3)-Si(1) and In(4)-Si(2). On the other hand, in the range from -7 to -4 eV, dispersive bands having large amplitude at the In atoms are originated from In-5 s orbitals, which contribute to the bondings between the In atoms.

Figure 4 shows the two-dimensional Fermi surfaces for the three metallic states at the surface. All of the states are empty on the left sides of the Fermi surfaces. The Fermi surfaces of $m2$ and $m3$ are approximately straight and parallel to the (4×1) direction, while that of $m1$ is warped and nearly closed at the M point. Here, the $m1$, $m2$, and $m3$ bands cross the Fermi level at $0.86\Gamma X - 0.98X'M$, $0.58\Gamma X - 0.62X'M$, and $0.46\Gamma X - 0.48X'M$, respectively. The fractions of electron occupation of each band are estimated as 0.08, 0.40, and 0.52 for the $m1$, $m2$, and $m3$ bands, respectively. These calculated Fermi surfaces are in excellent agreement with angle-resolved photoemission results that were obtained by Abukawa *et al.*¹⁶ What must be noted is that the Fermi surface of the $m3$ band nearly bisects the (4×1) Brillouin zone, showing a 1D-like metallic character along the chains. Hence, it can be said that the Fermi surface for the $m3$ band has the possibility of nesting. However, further theoretical, as well as experimental, investigations of the detailed electronic structures are necessary to reveal the true mechanism of the phase transition of this system.

In summary, we have performed the first theoretical calculations for the Si(111)- $(4 \times 1)\text{In}$ surface using the first-principles density-functional method. The optimized atomic coordinates and the calculated band structures agree well with the experimental results. As a result, we are able to conclusively support the structural model proposed by Bunk *et al.* However, in order to clarify the nature of the Peierls-like instabilities of this surface, much still remains to be done.

We acknowledge helpful discussions with Professor H.W. Yeom and Dr. T. Abukawa. The authors would like to express their thanks to Dr. J. Yamauchi for valuable suggestions concerning the computational method. Numerical calculations were performed on Fujitsu VPP700/E at RIKEN.

*Electronic address: junj@postman.riken.go.jp; Present address: Department of Electronic Engineering, The University of Electro-Communications, Chofu, Tokyo 182-8585, Japan

¹V. Derycke, P. Soukiassian, A. Mayne, G. Dujardin, and J. Gautier, Phys. Rev. Lett. **81**, 5868 (1998).

²M.M.R. Evans and J. Nogami, Phys. Rev. B **59**, 7644 (1999).

³K. Miki, D.R. Bowler, J.H.G. Owen, G.A.D. Briggs, and K. Sakamoto, Phys. Rev. B **59**, 14 868 (1999).

⁴S. Modesti, A. Falasca, M. Polentarutti, M.G. Betti, V.D. Renzi, and C. Mariani, Surf. Sci. **447**, 133 (2000).

- ⁵H.W. Yeom, S. Takeda, E. Rotenberg, I. Matsuda, K. Horikoshi, J. Schaefer, C.M. Lee, S.D. Kevan, T. Ohta, T. Nagao, and S. Hasegawa, *Phys. Rev. Lett.* **82**, 4898 (1999).
- ⁶C. Kumph, O. Bunk, J.H. Zeysing, Y. Su, M. Nielsen, R.L. Johnson, R. Feidenhans'l, and K. Bechgaard, *Phys. Rev. Lett.* **85**, 4916 (2000).
- ⁷J.J. Lander and J. Morrison, *Surf. Sci.* **2**, 553 (1964).
- ⁸A.A. Saranin, E.A. Khramtsova, K.V. Ignatovich, V.G. Lifshits, T. Numata, O. Kubo, M. Katayama, I. Katayama, and K. Oura, *Phys. Rev. B* **55**, 5353 (1997).
- ⁹M. Kawaji, S. Baba, and A. Kinbara, *Appl. Phys. Lett.* **34**, 748 (1979).
- ¹⁰H. Hirayama, S. Baba, and A. Kinbara, *Appl. Surf. Sci.* **33/34**, 193 (1988).
- ¹¹N. Nakamura, K. Anno, and S. Kono, *Surf. Sci.* **256**, 129 (1991).
- ¹²B.E. Steele, D.M. Cornelison, and L. Li, *Nucl. Instrum. Methods Phys. Res. B* **85**, 414 (1994).
- ¹³J.L. Stevens, M.S. Worthington, and I.S.T. Tsong, *Phys. Rev. B* **47**, 1453 (1993).
- ¹⁴H. Öfner, S.L. Surnev, Y. Shapira, and F.P. Netzer, *Phys. Rev. B* **48**, 10 940 (1993).
- ¹⁵T. Abukawa, M. Sasaki, F. Hisamatsu, M. Nakamura, T. Kinoshita, A. Kakizaki, T. Goto, and S. Kono, *J. Electron Spectrosc. Relat. Phenom.* **80**, 233 (1996).
- ¹⁶T. Abukawa, M. Sasaki, F. Hisamatsu, T. Goto, T. Kinoshita, A. Kakizaki, and S. Kono, *Surf. Sci.* **325**, 33 (1995).
- ¹⁷I.G. Hill and A.B. McLean, *Phys. Rev. B* **56**, 15 725 (1997).
- ¹⁸I.G. Hill and A.B. McLean, *Phys. Rev. Lett.* **82**, 2155 (1999).
- ¹⁹M.S. Finney, C. Norris, P.B. Howes, and E. Vlieg, *Surf. Sci.* **277**, 330 (1992).
- ²⁰M.S. Finney, C. Norris, P.B. Howes, M.A. James, J.E. Macdonald, A.D. Johnson, and E. Vlieg, *Physica B* **198**, 246 (1994).
- ²¹O. Bunk, G. Falkenberg, J.H. Zeysing, L. Lottermoser, R.L. Johnson, M. Nielsen, F. Berg-Rasmussen, J. Baker, and R. Feidenhans'l, *Phys. Rev. B* **59**, 12 228 (1999).
- ²²A.A. Saranin, A.V. Zotov, K.V. Ignatovich, V.G. Lifshits, T. Numata, O. Kubo, H. Tani, M. Katayama, and K. Oura, *Phys. Rev. B* **56**, 1017 (1997).
- ²³J. Nogami, S. -I Park, and C.F. Quate, *Phys. Rev. B* **36**, 6221 (1987).
- ²⁴J. Kraft, M.G. Ramsey, and F.P. Netzer, *Phys. Rev. B* **55**, 5384 (1997).
- ²⁵A.A. Saranin, A.V. Zotov, V.G. Lifshits, J.-T. Ryu, O. Kubo, H. Tani, T. Harada, M. Katayama, and K. Oura, *Phys. Rev. B* **60**, 14 372 (1999).
- ²⁶C. Collazo-Davila, L.D. Marks, K. Nishii, and Y. Tanishiro, *Surf. Rev. Lett.* **4**, 65 (1997).
- ²⁷T. Abukawa (private communication).
- ²⁸M. Tsukada *et al.*, computer program package TAPP, (University of Tokyo, Tokyo, Japan 1983-2001).
- ²⁹P. Hohenberg and W. Kohn, *Phys. Rev.* **136**, B864 (1964).
- ³⁰J.P. Perdew, K. Burke, and M. Ernzerhof, *Phys. Rev. Lett.* **77**, 3865 (1996).
- ³¹J.P. Perdew, K. Burke, and Y. Wang, *Phys. Rev. B* **54**, 16 533 (1996).
- ³²D.D. Koelling and B.N. Harmon, *J. Phys. C* **10**, 3107 (1977).
- ³³J.H. Wood and A.M. Boring, *Phys. Rev. B* **18**, 2701 (1978).
- ³⁴D. Vanderbilt, *Phys. Rev. B* **41**, 7892 (1990).
- ³⁵K. Laasonen, A. Pasquarello, R. Car, C. Lee, and D. Vanderbilt, *Phys. Rev. B* **47**, 10 142 (1993).
- ³⁶J. Yamauchi, M. Tsukada, S. Watanabe, and O. Sugino, *Surf. Sci.* **341**, L1037 (1995).
- ³⁷J. Yamauchi, M. Tsukada, S. Watanabe, and O. Sugino, *Phys. Rev. B* **54**, 5586 (1996).
- ³⁸S.G. Louie, S. Froyen, and M.L. Cohen, *Phys. Rev. B* **26**, 1738 (1982).